

Kernel quadrature by applying a point-wise gradient descent method to discrete energies

Ken'ichiro Tanaka^{*†}

February 24, 2021

Abstract

We propose a method for generating nodes for kernel quadrature by a point-wise gradient descent method. For kernel quadrature, most methods for generating nodes are based on the worst case error of a quadrature formula in a reproducing kernel Hilbert space corresponding to the kernel. In typical ones among those methods, a new node is chosen among a candidate set of points in each step by an optimization problem with respect to a new node. Although such sequential methods are appropriate for adaptive quadrature, it is difficult to apply standard routines for mathematical optimization to the problem. In this paper, we propose a method that updates a set of points one by one with a simple gradient descent method. To this end, we provide an upper bound of the worst case error by using the fundamental solution of the Laplacian on \mathbf{R}^d . We observe the good performance of the proposed method by numerical experiments.

Keywords Kernel quadrature, Point-wise gradient descent method, Discrete energy, Reproducing kernel Hilbert space, Gaussian kernel

Mathematics Subject Classification 65D30, 65D32, 65K05, 41A55, 41A63

1 Introduction

This paper is concerned with kernel quadrature, an approach to deriving numerical integration formulas with kernels. Let $d \in \mathbf{Z}_+$ be a positive integer, $\Omega \subset \mathbf{R}^d$ a region with a non-empty interior in \mathbf{R}^d , and μ a Borel measure on Ω . A formula for quadrature is formally expressed as

$$\int_{\Omega} f(x) d\mu(x) \approx \sum_{j=1}^N w_j f(x_j), \quad (1.1)$$

where $\mathcal{X}_N = \{x_1, \dots, x_N\} \subset \Omega$ and $\mathcal{W}_N = \{w_1, \dots, w_N\} \subset \mathbf{R}$ are the sets of distinct nodes and weights, respectively.

Besides Monte Carlo (MC) methods and quasi Monte Carlo (QMC) methods, kernels have been used to derive numerical integration formulas recently. There are several categories of

^{*}Department of Mathematical Informatics, Graduate School of Information Science and Technology, University of Tokyo. 7-3-1 Hongo, Bunkyo-ku, Tokyo, 113-8656, Japan. e-mail: kenichiro@mist.i.u-tokyo.ac.jp

[†]PRESTO, Japan Science and Technological Agency (JST), 4-1-8 Honcho, Kawaguchi-shi, Saitama, 332-0012, Japan.

such kernel methods. We can see a category of randomized methods for choosing nodes x_j . It includes importance sampling [8], random feature expansions [1], kernel quadrature with determinantal point processes (DPPs) [3], etc.

On the other hand, there are categories of deterministic methods. One of them consists of sequential algorithms choosing nodes x_j one-by-one with greedy ways. Such algorithms are kernel herding (KH) [2, 7], sequential Bayesian quadrature (SBQ) [10, 14], orthogonal matching pursuit (OMP) [14], and their variants [5, 6, 11, 12, 15, 16, 20]. For example, the SBQ is realized by the procedure

$$x_{N+1} \in \underset{x \in \Omega}{\operatorname{argmin}} (e^{\operatorname{wor}}(\mathcal{X}_N \cup \{x\}, \mathcal{W}_{N+1}^*; \mathcal{H}_K)) \quad (n = 1, 2, \dots), \quad (1.2)$$

where e^{wor} , \mathcal{W}_{N+1}^* , and \mathcal{H}_K denote an worst case error, optimal set of weights, and reproducing kernel Hilbert space defined later in (2.2), (3.1), and Section 2, respectively. The methods in this category are rational in that we can add new nodes with keeping existing nodes. Such procedures are useful for adaptive quadrature, which is useful in the case of a high-dimensional and/or complicated region Ω . However, each step like (1.2) requires nonlinear and nonconvex optimization choosing nodes among prepared ones in the region Ω .

There is another category of methods obtaining whole nodes at once. For example, Oettershagen [14] proposes a method solving nonlinear equation. Furthermore, Fekete points, which maximize the determinant of a kernel matrix, are known to be useful as nodes for quadrature. Unfortunately, it is hard to find them exactly because the maximization of the determinant is intractable in general. However, some approximate optimization methods have been proposed [13, 18], although these are aimed at approximation of functions. In fact, these optimization methods employ convex objective functions for finding a set of nodes. They enable us to find a good set of nodes by standard optimization routines without preparing a candidate set of nodes in Ω . In particular, a logarithmic energy with an external field

$$I(x_1, \dots, x_N) = \varepsilon^2 \sum_{k=1}^N x_k^2 + \sum_{1 \leq i < j \leq N} \log \frac{1}{|x_i - x_j|} \quad (1.3)$$

is derived in [13] as an objective function to find approximate Fekete points for a one-dimensional Gaussian kernel $K(x, y) = \exp(-\varepsilon^2(x - y)^2)$ with $\varepsilon > 0$. This tool is restricted to a one-dimensional Gaussian kernel and has the following problems:

1. It is difficult to extend it to higher-dimensional cases.
2. The relationship between it and the worst case error e^{wor} is unclear.

Therefore it would be useful for kernel quadrature if we can obtain an extension of the energy in (1.3) as an upper bound of the worst case error. Here we note that finding a set of nodes at once by optimization of such an extended energy may be difficult when we need to find very many nodes in very high-dimensional region Ω . However, in such a case, such an energy can be used also for a sequential algorithm finding nodes one-by-one.

In this paper, we provide an extension of the energy in (1.3) by using the fundamental solution of the Laplacian on \mathbf{R}^d and show that it provides an upper bound of the worst case error. A method for deriving these results is based on the idea of [17]. Based on the bound, we propose a method that updates a set of points one by one with a simple gradient descent

method, which we call a point-wise gradient descent method. This method does not require a candidate set of points in Ω and relatively easy to be implemented.

The rest of this paper is organized as follows. In Section 2, we review some basic notions for kernel quadrature. In Section 3, we review the basics about the energy in (1.3). In Section 4, we derive an extension of the energy by using the fundamental solution of the Laplacian on \mathbf{R}^d . In Section 5, we propose the point-wise gradient descent method. In Section 6, we show some results of numerical experiments. In Section 7, we conclude this paper.

2 Basic notions for kernel quadrature

Let $K : \Omega \times \Omega \rightarrow \mathbf{R}$ be a continuous and symmetric function and assume that it is positive definite. Let $\mathcal{H}_K(\Omega)$ be the reproducing kernel Hilbert space (RKHS) corresponding to the kernel K . It has the following properties:

1. $\forall x \in \Omega, K(\cdot, x) \in \mathcal{H}_K(\Omega)$,
2. $\forall f \in \mathcal{H}_K(\Omega), \forall x \in \Omega, \langle f, K(\cdot, x) \rangle_{\mathcal{H}_K} = f(x)$.

The latter is called a reproducing property. We consider quadrature formula (1.1) for a function $f \in \mathcal{H}_K(\Omega)$. This approximation can be regarded as that of the measure μ as follows:

$$\mu \approx \sum_{j=1}^N w_j \delta_{x_j}. \quad (2.1)$$

For the formula in (1.1), we can define the worst-case error $e^{\text{wor}}(\mathcal{X}_N, \mathcal{W}_N; \mathcal{H}_K)$ by

$$e^{\text{wor}}(\mathcal{X}_N, \mathcal{W}_N; \mathcal{H}_K) = \sup_{\substack{f \in \mathcal{H}_K \\ \|f\|_{\mathcal{H}_K} \leq 1}} \left| \int_{\Omega} f(x) dx - \sum_{i=1}^N w_i f(x_i) \right|. \quad (2.2)$$

In general, it is desirable to construct a good point set \mathcal{X}_N and weight set \mathcal{W}_N that make the worst-case error as small as possible. To approach this goal, the following well-known expression of the worst-case error is useful.

$$\begin{aligned} & (e^{\text{wor}}(\mathcal{X}_N, \mathcal{W}_N; \mathcal{H}_K))^2 \\ &= \left\| \int_{\Omega} K(y, x) d\mu(x) - \sum_{j=1}^N w_j K(y, x_j) \right\|_{\mathcal{H}_K}^2 \\ &= \int_{\Omega} \int_{\Omega} K(y, z) d\mu(y) d\mu(z) - 2 \sum_{j=1}^N w_j \int_{\Omega} K(x_j, x) d\mu(x) + \sum_{i=1}^N \sum_{j=1}^N w_i w_j K(x_i, x_j). \end{aligned} \quad (2.3)$$

This is owing to the reproducing property $\langle f, K(\cdot, x) \rangle_{\mathcal{H}_K} = f(x)$. Therefore sets \mathcal{X}_N and \mathcal{W}_N minimizing the value

$$-2 \sum_{j=1}^N w_j \int_{\Omega} K(x_j, x) d\mu(x) + \sum_{i=1}^N \sum_{j=1}^N w_i w_j K(x_i, x_j) \quad (2.4)$$

are required as a quadrature formula. We often assume that

$$w_i = \frac{1}{N} \quad (i = 1, \dots, N) \quad (2.5)$$

for simplicity.

3 Approximate Fekete points for Gaussian kernels

3.1 Expression of the worst case error by determinants

If we fix the point set \mathcal{X}_N , the right hand side in (2.3) becomes a quadratic form with respect to the weight set \mathcal{W}_N . Therefore, we can easily find its minimizer $\mathcal{W}_N^* = \{w_i^*\}$ as follows:

$$\mathbf{w}^* = \int_{\Omega} \mathcal{K}_{\mathcal{X}_N}^{-1} \mathbf{k}_{\mathcal{X}_N}(x) dx, \quad (3.1)$$

where $\mathbf{w}^* = (w_1^*, \dots, w_N^*)^T$, and

$$\mathcal{K}_{\mathcal{X}_N} = \begin{bmatrix} K(x_1, x_1) & K(x_1, x_2) & \cdots & K(x_1, x_N) \\ K(x_2, x_1) & K(x_2, x_2) & \cdots & K(x_2, x_N) \\ \vdots & \vdots & \ddots & \vdots \\ K(x_N, x_1) & K(x_N, x_2) & \cdots & K(x_N, x_N) \end{bmatrix}, \quad \mathbf{k}_{\mathcal{X}_N}(x) = \begin{bmatrix} K(x, x_1) \\ K(x, x_2) \\ \vdots \\ K(x, x_N) \end{bmatrix}. \quad (3.2)$$

By using these, we can express the worst-case error with the optimal weights \mathcal{W}_N^* by

$$(e^{\text{wor}}(\mathcal{X}_N, \mathcal{W}_N^*; \mathcal{H}_K))^2 = \frac{1}{\det \mathcal{K}_{\mathcal{X}_N}} \det \begin{bmatrix} k_0 & k_1 & \cdots & k_N \\ k_1 & & & \\ \vdots & & \mathcal{K}_{\mathcal{X}_N} & \\ k_N & & & \end{bmatrix}, \quad (3.3)$$

where

$$k_0 = \int_{\Omega} \int_{\Omega} K(x, y) dx dy, \quad k_i = \int_{\Omega} K(x, x_i) dx \quad (i = 1, \dots, n). \quad (3.4)$$

Clearly, the value $e^{\text{wor}}(\mathcal{X}_N, \mathcal{W}_N^*; \mathcal{H}_K)$ is less than or equal to the worst-case error with the equal weights in (2.5):

$$e^{\text{wor}}(\mathcal{X}_N, \mathcal{W}_N^*; \mathcal{H}_K) \leq e^{\text{wor}}(\mathcal{X}_N, \{1/N\}_{i=1}^N; \mathcal{H}_K). \quad (3.5)$$

According to Formula (3.3)¹, maximization of the determinant of the matrix $\mathcal{K}_{\mathcal{X}_N}$ seems to be useful, although we do not have some reasonable estimate of the worst case error for its maximizer: the Fekete points. Unfortunately, the maximization of $\det \mathcal{K}_{\mathcal{X}_N}$ is not tractable in general. However, in the case of the one-dimensional Gaussian kernel K , we can obtain a tractable approximation of the determinant by expanding the kernel [13].

¹Although its derivation is fundamental, we write it in Appendix A for readers' convenience.

3.2 Expansion and truncation of the one-dimensional Gaussian kernel

Let $K(x, y) := \exp(-\varepsilon^2|x - y|^2)$ be the one-dimensional Gaussian kernel. Then, we have

$$K(x, y) \approx \widehat{K}(x, y) = \sum_{\ell=0}^{n-1} \varphi_\ell(x)\varphi_\ell(y),$$

where $\varphi_\ell(x) := \exp(-\varepsilon^2 x^2) \sqrt{\frac{2^\ell \varepsilon^{2\ell}}{\ell!}} x^\ell$. Let $\widehat{\mathcal{K}}_{\mathcal{X}_N} = (\widehat{K}(x_k, x_m))_{k,m=1}^N \in \mathbf{R}^{n \times n}$ be the corresponding kernel matrix, where $\mathcal{X}_N = \{x_1, \dots, x_N\}$. Then, it is shown in [13] that

$$-\log(\det \widehat{\mathcal{K}}_{\mathcal{X}_N})^{1/2} = C_{\varepsilon, N} + \varepsilon^2 \sum_{k=1}^N x_k^2 + \sum_{1 \leq i < j \leq N} \log \frac{1}{|x_i - x_j|}, \quad (3.6)$$

where $C_{\varepsilon, N}$ is a constant independent of \mathcal{X}_N . This is the logarithmic energy with an external field shown in (1.3), for which we need to find a minimizer. We can show that this energy is convex and that there exists a unique minimiser $\mathcal{X}_N^* \in \mathcal{R}_N := \{(x_1, \dots, x_N) \in \Omega^N \mid x_1 < x_2 < \dots < x_{N-1} < x_N\}$. Therefore we can find \mathcal{X}_N^* numerically by using a standard optimization technique like the Newton method.

Unfortunately, extension of the above argument to higher-dimensional cases is difficult because of the complicated structure of the kernel matrix of the truncated kernel \widehat{K} for $d \geq 2$. Therefore we introduce another way for such extension in Section 4 below.

4 Bound for a discrete energy of the Gaussian kernel with the fundamental solution of the Laplacian

Taking the relation in (3.5) into account, we focus on the case of the equal weights in this section.

4.1 Discrete energy given by an integral of the heat kernel

Let $d \geq 2$. We use the d -dimensional fundamental solution $G_d(x, y)$ for the Laplacian Δ on \mathbf{R}^d . It is given by the following expression:

$$G_d(x, y) = \begin{cases} \frac{1}{2\pi} \log \|x - y\| & (d = 2), \\ -\frac{1}{2(d-2)s_d} \frac{1}{\|x - y\|^{d-2}} & (d \geq 3), \end{cases} \quad (4.1)$$

where s_d is the surface area of the $(d-1)$ dimensional unit sphere. The fundamental solution satisfies

$$\Delta_x G_d(x, y) = \delta_y(x) \quad (= \delta(x - y)). \quad (4.2)$$

The following lemmas are based on the ideas in [17], whereas their proofs are slightly different from those in the paper. Their proofs are provided in Section C.

Lemma 4.1. Let s and t be positive real numbers and let a and b be points in \mathbf{R}^d . Then the following equality holds:

$$\int_{\mathbf{R}^d} dx \int_{\mathbf{R}^d} dy G_d(x, y) e^{s\Delta_x} \delta_a(x) e^{t\Delta_y} \delta_b(y) = \int_{\mathbf{R}^d} dy G_d(a, y) e^{(s+t)\Delta_y} \delta_b(y).$$

Lemma 4.2. Let t be a positive real number and let b be a point in \mathbf{R}^d . Then, the value

$$\int_{\mathbf{R}^d} dy G_d(b, y) e^{t\Delta_y} \delta_b(y)$$

is bounded and depends only on d and t .

Lemma 4.3. Let t be a positive real number and let a and b be disjoint points in \mathbf{R}^d . Then the following equality holds:

$$\int_{\mathbf{R}^d} dy G_d(a, y) e^{t\Delta_y} \delta_b(y) = G_d(a, b) + \int_0^t \frac{1}{(4\pi s)^{d/2}} \exp\left(-\frac{\|a-b\|^2}{4s}\right) ds.$$

For a discrete measure

$$\mu_N = \frac{1}{N} \sum_{j=1}^N \delta_{x_j} \quad (4.3)$$

with disjoint sets $\{x_i\}_{i=1}^N$, we introduce a renormalized energy. To this end, for μ_N and a positive number $t > 0$, we define $A_d(t, \mu_N)$ by

$$A_d(t, \mu_N) := \int_{\mathbf{R}^d} dx \int_{\mathbf{R}^d} dy G_d(x, y) e^{\frac{t}{2}\Delta_x} \mu_N(x) e^{\frac{t}{2}\Delta_y} \mu_N(y). \quad (4.4)$$

Furthermore, we define a constant:

$$C_d(t) := \int_{\mathbf{R}^d} dy G_d(0, y) e^{t\Delta_y} \delta_0(y). \quad (4.5)$$

Then, we can derive the following relation by using the above lemmas.

Theorem 4.4. Let $t > 0$ be a positive number. Then, we have

$$\frac{1}{N^2} \sum_{i \neq j} \int_0^t \frac{1}{(4\pi s)^{d/2}} \exp\left(-\frac{\|x_i - x_j\|^2}{4s}\right) ds = A_d(t, \mu_N) - \frac{C_d(t)}{N} - \frac{1}{N^2} \sum_{i \neq j} G_d(x_i, x_j). \quad (4.6)$$

Proof. By using Lemmas 4.1, 4.2, and 4.3, we can derive the following equalities:

$$\begin{aligned} A_d(t, \mu_N) &= \frac{1}{N^2} \sum_{i=1}^N \sum_{j=1}^N \int_{\mathbf{R}^d} dx \int_{\mathbf{R}^d} dy G_d(x, y) e^{\frac{t}{2}\Delta_x} \delta_{x_i}(x) e^{\frac{t}{2}\Delta_y} \delta_{x_j}(y) \\ &= \frac{1}{N^2} \sum_{i=1}^N \sum_{j=1}^N \int_{\mathbf{R}^d} dy G_d(x_i, y) e^{t\Delta_y} \delta_{x_j}(y) \quad (\because \text{Lemma 4.1}) \\ &= \frac{1}{N^2} \left(\sum_{i=j} + \sum_{i \neq j} \right) \int_{\mathbf{R}^d} dy G_d(x_i, y) e^{t\Delta_y} \delta_{x_j}(y) \end{aligned}$$

$$= \frac{C_d(t)}{N} + \frac{1}{N^2} \sum_{i \neq j} \left\{ G_d(x_i, x_j) + \int_0^t \frac{1}{(4\pi s)^{d/2}} \exp\left(-\frac{\|x_i - x_j\|^2}{4s}\right) ds \right\}$$

(\because Lemmas 4.2 and 4.3).

Hence the conclusion follows. □

Here we present a sketch of an idea to estimate both sides of (4.6). Suppose that

- the points x_j are in a bounded region $\Omega \subset B[0, r] \subset \mathbf{R}^d$, and
- t is sufficiently large so that $A_d(t, \mu_N)$ is almost independent of $\{x_j\}_{j=1}^N$.

Under these conditions, we may have

$$\begin{aligned} & \int_0^t \frac{1}{(4\pi s)^{d/2}} \exp\left(-\frac{\|x_i - x_j\|^2}{4s}\right) ds \\ &= \left(\int_0^r + \int_r^t \right) \frac{1}{(4\pi s)^{d/2}} \exp\left(-\frac{\|x_i - x_j\|^2}{4s}\right) ds \\ &\approx \int_0^r \frac{1}{(4\pi s)^{d/2}} \exp\left(-\frac{\|x_i - x_j\|^2}{4s}\right) ds + \int_r^t \frac{1}{(4\pi s)^{d/2}} ds \end{aligned} \quad (4.7)$$

$$\approx \hat{C}_{d,r} \exp\left(-\frac{\|x_i - x_j\|^2}{4r}\right) + \int_r^t \frac{1}{(4\pi s)^{d/2}} ds. \quad (4.8)$$

Therefore we may state that the terms depending on $\{x_j\}_{j=1}^N$ in (4.6) are:

- $\frac{1}{N^2} \sum_{i \neq j} \hat{C}_{d,r} \exp\left(-\frac{\|x_i - x_j\|^2}{4r}\right)$ (in the LHS) and
- $-\frac{1}{N^2} \sum_{i \neq j} G_d(x_i, x_j)$ (in the RHS).

We make the above rough idea rigorous in Section 4.2 below. That is, we derive a bound of the energy of the Gaussian kernel by using Theorem 4.4.

4.2 Bound of the discrete energy of the Gaussian kernel

We provide a lower bound of the integral of the heat kernel in Theorem 4.4 by the following lemma, whose proof is provided in Section C.

Lemma 4.5. Let $\Omega \subset \mathbf{R}^d$ be a bounded region with $D := \text{diam } \Omega < \infty$ and let $x, y \in \Omega$ be disjoint points in the region. Then, for any t with $t \geq D^2/d$, we have

$$\int_0^t \frac{1}{(4\pi s)^{d/2}} \exp\left(-\frac{\|x - y\|^2}{4s}\right) ds \geq \frac{1}{(4\pi)^{d/2}} \left[\frac{d^{d/2-1}}{2D^{d-2}} \exp\left(-\frac{d\|x - y\|^2}{4D^2}\right) + h_{d,D}(t) \right], \quad (4.9)$$

where

$$h_{d,D}(t) := \begin{cases} \frac{e^{-d/4}}{1 - d/2} \left(\frac{1}{t^{d/2-1}} - \frac{d^{d/2-1}}{D^{d-2}} \right) & (d \neq 2), \\ e^{-1/2} \log\left(\frac{2t}{D^2}\right) & (d = 2). \end{cases} \quad (4.10)$$

Remark 4.1. The function $h_{d,D}$ in (4.10) satisfies $h_{d,D}(t) \geq 0$ for any t with $t \geq D^2/d$.

By combining Theorem 4.4 and Lemma 4.5, we have the following estimate of the energy of the Gaussian kernel.

Theorem 4.6. Let $\Omega \subset \mathbf{R}^d$ be a bounded region with $D := \text{diam } \Omega < \infty$. Let $\{x_i\}_{i=1}^N \subset \Omega$ be a set of disjoint points in Ω and let μ_N be the discrete measure given by (4.3). Then, for any t with $t \geq D^2/d$ and a with $a \geq \sqrt{d}/(2D)$, we have

$$\begin{aligned} & \frac{1}{N^2} \sum_{i \neq j} \exp(-a^2 \|x_i - x_j\|^2) \\ & \leq \frac{2(4\pi)^{d/2} D^{d-2}}{d^{d/2-1}} \left(-\frac{1}{N^2} \sum_{i \neq j} G_d(x_i, x_j) + A_d(t, \mu_N) - \frac{C_d(t)}{N} - \frac{1}{(4\pi)^{d/2}} \frac{N-1}{N} h_{d,D}(t) \right), \end{aligned} \quad (4.11)$$

where $A_d(t, \mu_N)$ and $C_d(t)$ are given by (4.4) and (4.5), respectively.

Proof. It follows from inequality (4.9) in Lemma 4.5 and equality (4.6) in Theorem 4.4 that

$$\begin{aligned} & \frac{1}{N^2} \sum_{i \neq j} \frac{1}{(4\pi)^{d/2}} \frac{d^{d/2-1}}{2D^{d-2}} \exp(-a^2 \|x_i - x_j\|^2) \\ & \leq \frac{1}{N^2} \sum_{i \neq j} \frac{1}{(4\pi)^{d/2}} \frac{d^{d/2-1}}{2D^{d-2}} \exp\left(-\frac{d \|x_i - x_j\|^2}{4D^2}\right) \\ & \leq \frac{1}{N^2} \sum_{i \neq j} \int_0^t \frac{1}{(4\pi s)^{d/2}} \exp\left(-\frac{\|x_i - x_j\|^2}{4s}\right) ds - \frac{1}{(4\pi)^{d/2}} \frac{N-1}{N} h_{d,D}(t) \\ & = A_d(t, \mu_N) - \frac{C_d(t)}{N} - \frac{1}{N^2} \sum_{i \neq j} G_d(x_i, x_j) - \frac{1}{(4\pi)^{d/2}} \frac{N-1}{N} h_{d,D}(t). \end{aligned}$$

Thus we have the conclusion. \square

In the parenthesis of the RHS of (4.11), the second term $A_d(t, \mu_N)$ also depends on the set $\{x_i\}_{i=1}^N$. However, we can expect that the dependence tends to disappear as $t \rightarrow \infty$. Therefore minimization of

$$-\frac{1}{N^2} \sum_{i \neq j} G_d(x_i, x_j)$$

will provide approximate minimizer of the energy of the Gaussian kernel.

5 Approximate minimization of the worst case error by a point-wise gradient descent method

In this section, we present a method for generating points for quadrature based on the arguments in Section 4. Then, based on the relation in (3.5), we compute the optimal weights by using Formula (3.1) to obtain a quadrature formula.

5.1 Objective functions

According to Theorem 4.6, we can provide an upper bound of the value in (2.4) in the case of the Gaussian kernel $K(x, y) = \exp(-a^2\|x - y\|^2)$ with $a \geq \sqrt{d}/(2D)$. That is, the value

$$\begin{aligned}
 & -\frac{2}{N} \sum_{j=1}^N \int_{\Omega} K(x_j, x) \, d\mu(x) - \frac{\hat{C}_{d,D}}{N^2} \sum_{i \neq j} G_d(x_i, x_j) \\
 & \quad + \hat{C}_{d,D} \left(A_d(t, \mu_N) - \frac{C_d(t)}{N} - \frac{1}{(4\pi)^{d/2}} \frac{N-1}{N} h_{d,D}(t) \right)
 \end{aligned} \tag{5.1}$$

is such an upper bound, where

$$\hat{C}_{d,D} := \frac{2(4\pi)^{d/2} D^{d-2}}{d^{d/2-1}}.$$

Since the underlined part of (5.1) is almost independent of the set $\{x_j\}_{j=1}^N$, we minimize the other part of (5.1) to obtain an approximate minimizer of the worst case error. In the following, we deal with the Gaussian kernel $K(x, y) = \exp(-\|x - y\|^2)$. That is, we consider the case that $a = 1$ in Theorem 4.6. Let $J_1(x)$ be defined by

$$J_1(x) := \int_0^1 \exp(-|x - y|^2) \, dx = \frac{\sqrt{\pi}}{2} (\operatorname{erf}(1 - x) + \operatorname{erf}(x)).$$

In the following, we consider the two and three dimensional cases.

5.1.1 Two dimensional case: $d = 2$

We consider a region $\Omega = [0, 1]^2$ and measure $d\mu(x) = dx$. Then, we have $D = \sqrt{2}$ and $\hat{C}_{d,D} = 8\pi$, and we can confirm that $a = 1 \geq 1/2 = \sqrt{d}/(2D)$. Furthermore, we have

$$\int_{\Omega} K(x, y) \, d\mu(y) = J_1(x^{(1)})J_1(x^{(2)}) =: J_2(x), \tag{5.2}$$

where $x^{(1)}$ and $x^{(2)}$ are the first and second components of $x \in [0, 1]^2$, respectively. From these and the two-dimensional fundamental solution in (4.1), the objective function in (5.1) is written in the form

$$I_2(x_1, \dots, x_N) := -\frac{2}{N} \sum_{j=1}^N J_2(x_j) + \frac{4}{N^2} \sum_{i \neq j} \log \frac{1}{\|x_i - x_j\|}. \tag{5.3}$$

5.1.2 Three dimensional case: $d = 3$

We consider a region $\Omega = [0, 1]^3$ and measure $d\mu(x) = dx$. Then, we have $D = \sqrt{3}$ and $\hat{C}_{d,D} = 16\pi^{3/2}$, and we can confirm that $a = 1 \geq 1/2 = \sqrt{d}/(2D)$. Furthermore, we have

$$\int_{\Omega} K(x, y) \, d\mu(y) = J_1(x^{(1)})J_1(x^{(2)})J_1(x^{(3)}) =: J_3(x), \tag{5.4}$$

where $x^{(1)}$, $x^{(2)}$ and $x^{(3)}$ are the first, second and third components of $x \in [0, 1]^3$, respectively. From these and the three-dimensional fundamental solution in (4.1), the objective function in (5.1) is written in the form

$$I_3(x_1, \dots, x_N) := -\frac{2}{N} \sum_{j=1}^N J_3(x_j) + \frac{2\sqrt{\pi}}{N^2} \sum_{i \neq j} \frac{1}{\|x_i - x_j\|}. \quad (5.5)$$

Remark 5.1. The functions I_2 and I_3 are similar to the Riesz energies (see e.g. [4]), which have an intrinsic repelling property. As shown in Section 6, this property seems to be well-suited to a method introduced in Section 5.3. Similar energies are considered and different algorithms are applied to them in [11, 12].

5.2 Regularization terms

In the functions I_2 and I_3 , the sums of $J_2(x_j)$ and $J_3(x_j)$ take roles as regularization terms, respectively. However, it was observed that their effects were so weak that minimization of I_2 and I_3 made points x_j accumulate near the boundary of Ω . Since such distribution is not appropriate for quadrature on Ω , we introduce stronger regularization terms.

To this end, we begin with approximating the characteristic functions of the regions $[0, 1]^2$ and $[0, 1]^3$:

$$\delta_{[0,1]^d}(x) := \begin{cases} 0 & (x \in [0, 1]^d), \\ \infty & (x \notin [0, 1]^d), \end{cases} \quad (d = 2, 3).$$

There are various choices about such approximate functions. In this paper, by using a real number $M > 0$, we choose

$$\begin{aligned} \tilde{\delta}_M^{(2)}(x) &:= \sum_{\ell=1}^2 \left(\log \frac{1}{x^{(\ell)} - M} + \log \frac{1}{1 + M - x^{(\ell)}} \right) \quad \text{and} \\ \tilde{\delta}_M^{(3)}(x) &:= \sum_{\ell=1}^3 \left(\frac{1}{x^{(\ell)} - M} + \frac{1}{1 + M - x^{(\ell)}} \right) \end{aligned}$$

for $\delta_{[0,1]^2}(x)$ and $\delta_{[0,1]^3}(x)$, respectively. The number M sets a margin of the boundaries of the regions. By using these, we introduce

$$R_2(x_1, \dots, x_N) := \frac{1}{N^P} \sum_{i=1}^N \tilde{\delta}_M^{(2)}(x_i) \quad \text{and} \quad (5.6)$$

$$R_3(x_1, \dots, x_N) := \frac{1}{N^P} \sum_{i=1}^N \tilde{\delta}_M^{(3)}(x_i) \quad (5.7)$$

as regularization terms in the cases of $d = 2$ and $d = 3$, respectively. The parameter P determines strength of these terms.

We generate a set $\{x_j\}$ of points by minimizing the functions

$$I_d(x_1, \dots, x_N) + R_d(x_1, \dots, x_N) \quad (d = 2, 3).$$

The hyper-parameters P and M are chosen so that good distribution of points are obtained by the algorithm proposed below in Section 5.3.

Remark 5.2. The functions $\tilde{\delta}_M^{(2)}$ and $\tilde{\delta}_M^{(3)}$ are not based on any theory, although they imitates the corresponding fundamental solutions. In addition, the factor N^{-P} in (5.6) and (5.7) may have room for improvement. Finding more appropriate regularization terms based on a theory is a topic for future work.

Remark 5.3. In [9], the authors use the heat kernels, which are time-dependent Gaussian kernels in a special case, to generate points on compact manifolds via simulated annealing. They show superiority of the points given by the heat kernels over those given by the Riesz kernels and other QMC sequences. In Section 6 of this paper, we observe that the functions I_d with the regularization terms R_d can be superior to the functions of the worst case error for the Gaussian kernel.

5.3 Point-wise gradient descent method (PWGD)

Here we propose an algorithm for generating a set $\{x_j\}$ of points by using the function $I_d + R_d$. We intend to realize a so simple algorithm with cheap computational cost that it can be applied to high-dimensional cases with many points. To this end, it is better to avoid preparation of many candidate points in Ω among which points for quadrature are selected.

Taking these considerations into account, we propose Algorithm 1 for generating points for quadrature. We call it a point-wise gradient descent method (PWGD). After preparing an initial set $\{x_j\}_{j=1}^N \subset \Omega$, the algorithm updates its member one by one with a gradient of the function $I_d + R_d$ with respect to the member.

Algorithm 1 Point-wise gradient descent method (PWGD)

Require: a number N of points, a default step size $\gamma > 0$

Ensure: a set $\{x_i\}_{i=1}^N \subset \Omega$ of points

```

1: generate an initial set  $\{x_i\}_{i=1}^N \subset \Omega$  randomly
2: for  $k = 1, \dots, K_{\max}$  do
3:   for  $i = 1, \dots, N$  do
4:      $g_i := \nabla_{x_i} \{I_d(x_1, \dots, x_N) + R_d(x_1, \dots, x_N)\}$ 
5:      $\gamma' := \max\{\beta \geq 0 \mid x_i - \beta g_i \in \Omega\}$ 
6:      $\gamma \leftarrow \max\{\gamma, \gamma'\}$ 
7:      $x_i \leftarrow x_i - \gamma g_i$ 
8:   end for
9:   if  $\max_{1 \leq i \leq N} \|g_i\| < \epsilon$  then
10:    break
11:   end if
12: end for
13: return  $\{x_i\}_{i=1}^N$ 

```

Finally, we obtain a set $\{(x_j, w_j^*)\}_{j=1}^N$ of points and weights for quadrature by the following procedure.

1. Obtain a set $\{x_j\}_{j=1}^N \subset \Omega$ by Algorithm 1 (PWGD) with equal weights: $w_j = 1/N$.
2. Compute the optimal weights $\{w_j^*\}_{j=1}^N$ by Formula (3.3): $\mathbf{w}^* = \int_{\Omega} \mathcal{K}_{\mathcal{X}_N}^{-1} \mathbf{k}_{\mathcal{X}_N}(x) d\mu(x)$.

6 Numerical experiments

We compute the sets $\{(x_j, w_j^*)\}_{j=1}^N$ by the proposed procedure in the cases that $K(x, y) = \exp(-\|x - y\|^2)$ and $\Omega = [0, 1]^d$ for $d = 2, 3$. We set $\gamma = 1$ in Algorithm 1 and choose the hyper-parameters P and M experimentally. For comparison, we also use other methods shown below:

M1 Sequential Bayesian quadrature (SBQ),

M2 Application of the point-wise gradient descent method to the worst-case error with the equal weights: $e^{\text{wor}}(\mathcal{X}_N, \{1/N\}_{i=1}^N; \mathcal{H}_K)$.

In particular, we deal with the latter method to confirm the effect of the proposed method. We set $\gamma = 0.1$ in Algorithm 1². In addition, we used $\varepsilon = 10^{-5}$ and $\varepsilon = 10^{-4}$ in Algorithm 1 in the cases of $d = 2$ and $d = 3$, respectively.

MATLAB programs are used for all computation in this section. In addition, the computation is done with the double precision floating point numbers. The programs used for the computation are available on the web page [19].

6.1 Two dimensional case: $d = 2$

First, we show the generated points in Figures 1–4. We can observe that the points given by the proposed procedure are separated each other and do not gather around a certain point as opposed to those given by the other methods.

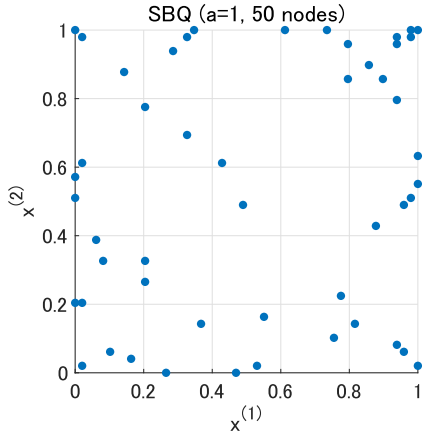


Figure 1: 50 points given by M1 (SBQ).

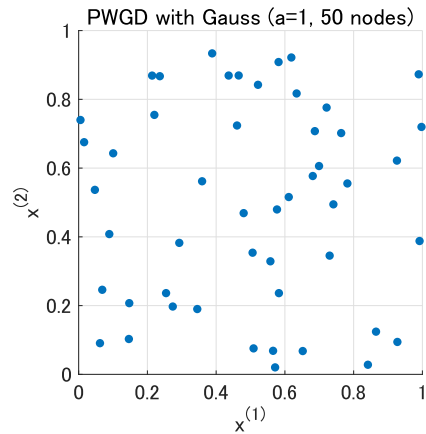


Figure 2: 50 points given by M2 (PWGD for the original worst-case error).

²The default step size γ in Algorithm 1 is determined experimentally. In most cases, we observed that the inner iteration was terminated before it reached the maximum number K_{\max} of the iteration.

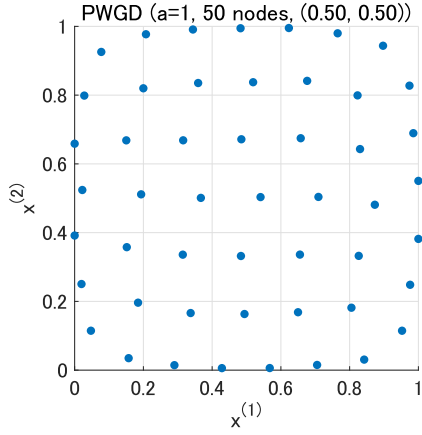


Figure 3: 50 points given by the proposed procedure with $(P, M) = (0.5, 0.5)$.

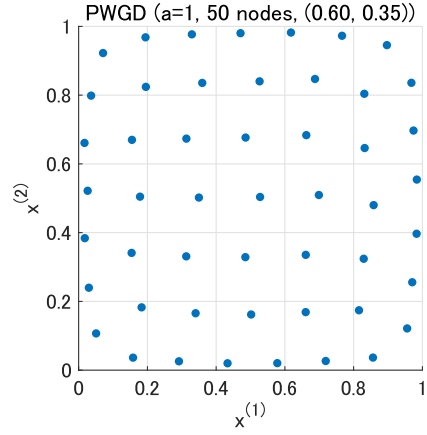


Figure 4: 50 points given by the proposed procedure with $(P, M) = (0.6, 0.35)$.

Next, in Figures 5 and 6, we show the worst case errors for the points and weights given by methods M1, M2 and the proposed procedure. We can observe that the proposed procedure outperforms with the other methods when the hyper-parameters (P, M) are set appropriately according to N , the number of the points.

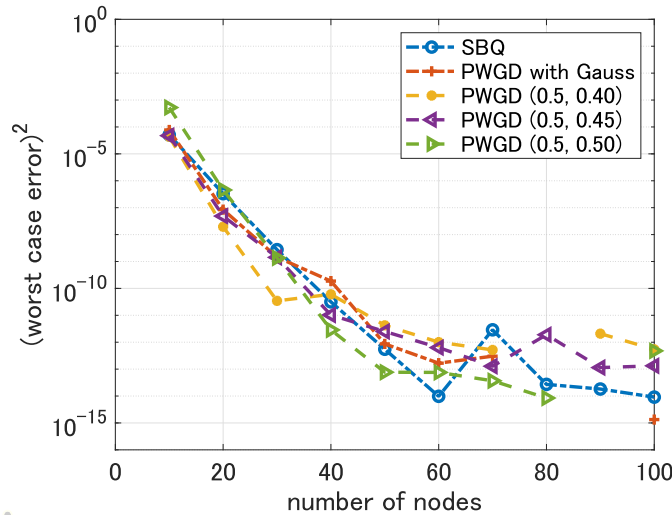


Figure 5: Squared worst case errors. The horizontal axis corresponds to N . The legend “PWGD with Gauss” indicates method M2 and “PWGD (P, M) ” indicates the proposed procedure with the hyper-parameters (P, M) . Here $P = 0.5$.

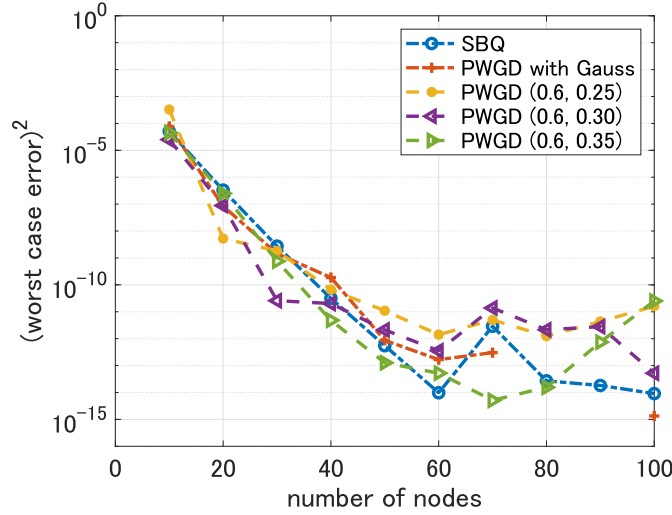


Figure 6: Squared worst case errors. The horizontal axis corresponds to N . The legend “PWGD with Gauss” indicates method M2 and “PWGD (P, M) ” indicates the proposed procedure with the hyper-parameters (P, M) . Here $P = 0.6$.

6.2 Three dimensional case: $d = 3$

First, we show the generated points in Figures 7–10. We can observe similar situations to the two-dimensional case.

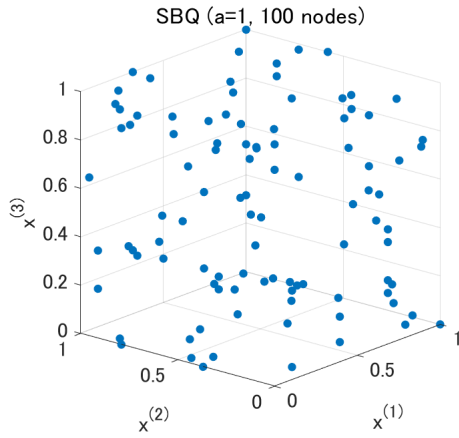


Figure 7: 100 points given by M1 (SBQ).

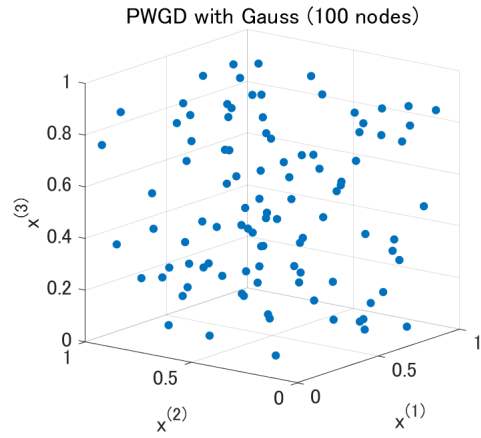


Figure 8: 100 points given by M2 (PWGD for the original worst-case error).

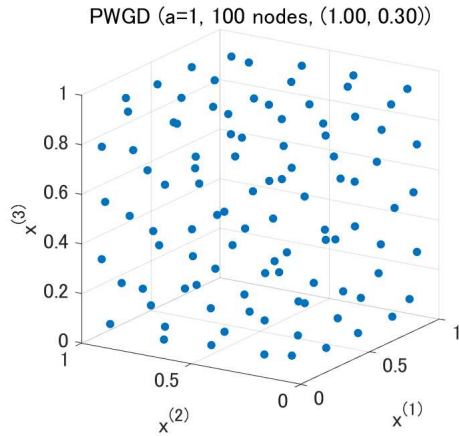


Figure 9: 100 points given by the proposed procedure with $(P, M) = (1.0, 0.3)$.

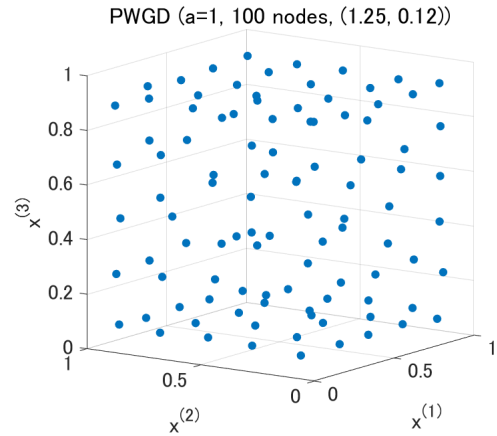


Figure 10: 100 points given by the proposed procedure with $(P, M) = (1.25, 0.12)$.

Next, in Figures 11 and 12, we show the worst case errors for the points and weights given by methods M1, M2 and the proposed procedure. We can observe that the proposed procedure often outperforms method M2, which implies that the proposed function $I_d + R_d$ is well-suited to the point-wise gradient descent algorithm. On the other hand, the performance of the proposed procedure seems to be slightly worse than that of method M1 (SBQ), although the former outperforms the latter in some cases.

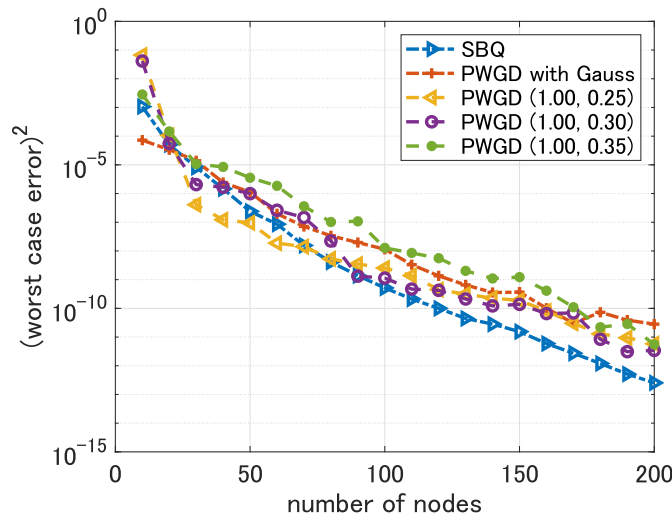


Figure 11: Squared worst case errors. The horizontal axis corresponds to N . The legend “PWGD with Gauss” indicates method M2 and “PWGD (P, M) ” indicates the proposed procedure with the hyper-parameters (P, M) . Here $P = 1.0$.

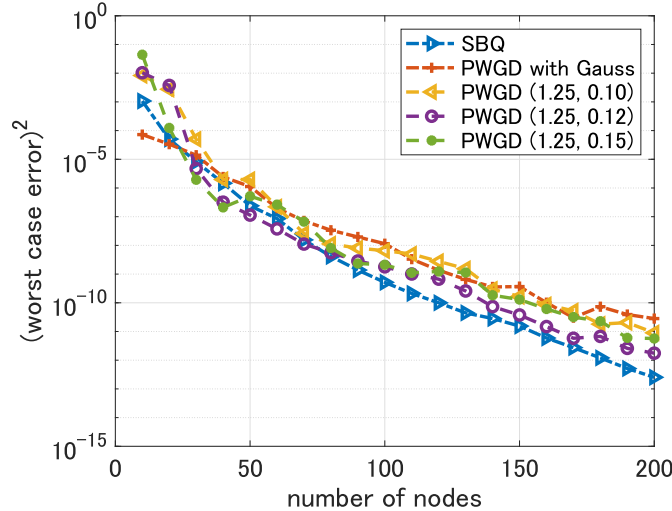


Figure 12: Squared worst case errors. The horizontal axis corresponds to N . The legend “PWGD with Gauss” indicates method M2 and “PWGD (P, M) ” indicates the proposed procedure with the hyper-parameters (P, M) . Here $P = 1.25$.

7 Concluding remarks

By using the fundamental solutions of the Laplacian on \mathbf{R} , we have provided the upper bound in (5.1) for the main terms in (2.4) of the worst case error in an RKHSs with the Gaussian kernel. Based on the bound, we have proposed the objective functions with the regularization terms and Algorithm 1 (PWGD) for generating points for quadrature in Section 5. Then, quadrature formulas are obtained by calculating the optimal weights with respect to the generated points. By the numerical experiments in Section 6, we have observed that this procedure can outperform the SBQ and PWGD with the original worst case error if the hyper-parameters are appropriate. We can guess that direct application of the PWGD to the original worst case error tends to make a set of points trapped in a bad local minimum.

We mention some topics for future work. Since the upper bound in (5.1) is loose and the regularization terms are artificial, it will be better to find discrete energies that is more suited to the PWGD. After that, theoretical guarantee of the performance of the PWGD should be required. Furthermore, we will consider generalization of such results to other kernels.

Acknowledgements

This work was partly supported by JST, PRESTO Grant Number JPMJPR2023, Japan.

References

- [1] Bach, F.: On the equivalence between kernel quadrature rules and random feature expansions. *The Journal of Machine Learning Research*, 18, 714–751 (2017)

- [2] Bach, F., Lacoste-Julien, S., and Obozinski, G.: On the equivalence between herding and conditional gradient algorithms. *ICML'12: Proceedings of the 29th International Conference on International Conference on Machine Learning* 1355–1362 (2012)
- [3] Belhadji, A., Bardenet, R., and Chainais, P.: Kernel quadrature with DPPs. In: *Advances in Neural Information Processing Systems*, 12927–12937 (2019)
- [4] Brauchart, J. S., and Grabner, P. J.: Distributing many points on spheres: Minimal energy and designs. *J. Complexity* 31, 293–326 (2015)
- [5] Briol, F.-X., Oates, C., Girolami, M., and Osborne, M.: Frank-Wolfe Bayesian quadrature: Probabilistic integration with theoretical guarantees. In *Advances in Neural Information Processing Systems*, 1162–1170 (2015)
- [6] Chen, W., Mackey, L., Gorham, J., Briol, F.-X., and Oates, C.: Stein points. In *Proceedings of the 35th International Conference on Machine Learning*, PMLR 80, 844–853 (2018)
- [7] Chen, Y., Welling, M., and Smola A.: Super-samples from kernel herding. In *Proceedings of the 26th Conference on Uncertainty in Artificial Intelligence*, UAI'10, 109–116, Arlington, Virginia, United States, AUAI Press (2010)
- [8] Liu, Q., and Lee, J. D.: Black-box importance sampling. In *Proceedings of the 20th International Conference on Artificial Intelligence and Statistics (AISTATS)*, PMLR 54, 952-961 (2017)
- [9] Lu, J., Sachs, M., and Steinerberger, S.: Quadrature points via heat kernel repulsion. *Constr. Approx.* 51, 27–48 (2020)
- [10] Huszár, F., and Duvenaud, D.: Optimally-weighted herding is Bayesian quadrature. *UAI'12: Proceedings of the Twenty-Eighth Conference on Uncertainty in Artificial Intelligence* 377–386 (2012)
- [11] Joseph, V., Dasgupta, T., Tuo, R., and Wu, C.: Sequential exploration of complex surfaces using minimum energy designs. *Technometrics*, 57(1), 64–74 (2015)
- [12] Joseph, V., Wang, D., Gu, L., Lyu, S., and Tuo, R.: Deterministic sampling of expensive posteriors using minimum energy designs. *Technometrics*, 61(3), 297–308 (2019)
- [13] Karvonen, T., Särkkä, S., and Tanaka, K.: Kernel-based interpolation at approximate Fekete points. *Numer. Algor.* (2020)
- [14] Oettershagen, J.: Construction of optimal cubature algorithms with applications to econometrics and uncertainty quantification. Ph. D. thesis, Institut für Numerische Simulation, Universität Bonn (2017)
- [15] Pronzato, L. and Zhigljavsky, A.: Bayesian quadrature, energy minimization and space-filling design. *SIAM/ASA J. Uncertainty Quantification*, 8(3), 959–1011 (2020)
- [16] Pronzato, L. and Zhigljavsky, A.: Minimum-energy measures for singular kernels. *Journal of Computational and Applied Mathematics* 382, 113089 (2021)

- [17] Steinerberger, S.: On the logarithmic energy of points on \mathbb{S}^2 . arXiv:2011.04630 (2020)
- [18] Tanaka, K.: Generation of point sets by convex optimization for interpolation in reproducing kernel Hilbert spaces. Numer. Algor. 84, 1049–1079 (2020)
- [19] Tanaka, K.: Matlab programs for a point-wise gradient descent method for kernel quadrature. https://github.com/KeTanakaN/mat_PWGD_for_KQ (last accessed on February 21, 2021)
- [20] Teymur, O., Gorham, J., Riabiz, M., and Oates, C.: Optimal quantisation of probability measures using maximum mean discrepancy. In Proceedings of the 24th International Conference on Artificial Intelligence and Statistics (AISTATS), PMLR 130 (2021)

A Derivation of Formula (3.3)

Note that the right hand side of (2.3) is rewritten in the form

$$\int_{\Omega} \int_{\Omega} K(x, y) \, dx dy - 2 \int_{\Omega} \mathbf{w}^T \mathbf{k}_{\mathcal{X}_N}(x) \, dx + \mathbf{w}^T \mathcal{K}_{\mathcal{X}_N} \mathbf{w} \quad (\text{A.1})$$

by using $\mathbf{w} = (w_1, \dots, w_N)^T$. Then, by letting $\mathbf{w} = \mathbf{w}^*$ in (A.1), we have

$$\begin{aligned} & \int_{\Omega} \int_{\Omega} K(x, y) \, dx dy - 2 \int_{\Omega} \mathbf{w}^T \mathbf{k}_{\mathcal{X}_N}(x) \, dx + \mathbf{w}^T \mathcal{K}_{\mathcal{X}_N} \mathbf{w} \\ &= \int_{\Omega} \int_{\Omega} K(x, y) \, dx dy - \int_{\Omega} \int_{\Omega} (\mathbf{k}_{\mathcal{X}_N}(x))^T \mathcal{K}_{\mathcal{X}_N}^{-1} \mathbf{k}_{\mathcal{X}_N}(y) \, dx \, dy \\ &= \int_{\Omega} \int_{\Omega} K(x, y) \, dx dy + \frac{1}{\det \mathcal{K}_{\mathcal{X}_N}} \det \left[\begin{array}{c|ccc} 0 & k_1 & \cdots & k_N \\ \hline k_1 & & & \\ \vdots & & & \\ k_N & & & \mathcal{K}_{\mathcal{X}_N} \end{array} \right] \\ &= \frac{1}{\det \mathcal{K}_{\mathcal{X}_N}} \det \left[\begin{array}{c|ccc} k_0 & k_1 & \cdots & k_N \\ \hline k_1 & & & \\ \vdots & & & \\ k_N & & & \mathcal{K}_{\mathcal{X}_N} \end{array} \right]. \end{aligned}$$

B Integrability of the fundamental solutions of the Laplacian

Regard the fundamental solution $G(x, y)$ in (4.1) as a function of x for a fixed y . Then, for $d \geq 2$, it has a singularity at $x = y$. Here we confirm that it is integrable on a bounded neighborhood of the singularity. In the following, we assume that $y = 0$ without loss of generality. Let $B_d[0, R] := \{x \in \mathbf{R}^d \mid \|x\| \leq R\}$ be a closed ball.

B.1 $d = 2$

We assume that $R \leq 1$. Then, we have

$$\int_{B_2[0, R]} |G_2(x, 0)| \, dx = - \int_0^R r \, dr \int_0^{2\pi} d\theta \frac{1}{2\pi} \log r = -\frac{R^2}{4} (2 \log R - 1) < \infty.$$

B.2 $d \geq 3$

We have

$$\int_{B_d[0,R]} |G_d(x,0)| dx = \int_0^R r^{d-1} dr \cdot s_d \cdot \frac{1}{2(d-2)s_d} \frac{1}{r^{d-2}} = \frac{R^2}{4(d-2)} < \infty.$$

C Proofs

Proof of Lemma 4.1. By integration by parts and equality (4.2), we have

$$\begin{aligned} \frac{\partial}{\partial s}(\text{LHS}) &= \int_{\mathbf{R}^d} dy e^{t\Delta_y} \delta_b(y) \int_{\mathbf{R}^d} dx G_d(x,y) \Delta_x e^{s\Delta_x} \delta_a(x) \\ &= \int_{\mathbf{R}^d} dy e^{t\Delta_y} \delta_b(y) \int_{\mathbf{R}^d} dx \Delta_x G_d(x,y) e^{s\Delta_x} \delta_a(x) \\ &= \int_{\mathbf{R}^d} dy e^{t\Delta_y} \delta_b(y) \int_{\mathbf{R}^d} dx \delta_y(x) e^{s\Delta_x} \delta_a(x) \\ &= \int_{\mathbf{R}^d} dy e^{t\Delta_y} \delta_b(y) e^{s\Delta_y} \delta_a(y) \\ &= \int_{\mathbf{R}^d} dy e^{(s+t)\Delta_y} \delta_b(y) \delta_a(y), \end{aligned}$$

and

$$\begin{aligned} \frac{\partial}{\partial s}(\text{RHS}) &= \int_{\mathbf{R}^d} dy G_d(a,y) \Delta_y e^{(s+t)\Delta_y} \delta_b(y) \\ &= \int_{\mathbf{R}^d} dy \Delta_y G_d(a,y) e^{(s+t)\Delta_y} \delta_b(y) \\ &= \int_{\mathbf{R}^d} dy \delta_a(y) e^{(s+t)\Delta_y} \delta_b(y). \end{aligned}$$

Therefore they coincide. Furthermore, by taking the limit of both sides as $s \rightarrow +0$, we have

$$\begin{aligned} \lim_{s \rightarrow +0} (\text{LHS}) &= \int_{\mathbf{R}^d} dx \int_{\mathbf{R}^d} dy G_d(x,y) \delta_a(x) e^{t\Delta_y} \delta_b(y) \\ &= \int_{\mathbf{R}^d} dy e^{t\Delta_y} \delta_b(y) \int_{\mathbf{R}^d} dx G_d(x,y) \delta_a(x) \\ &= \int_{\mathbf{R}^d} dy e^{t\Delta_y} \delta_b(y) G_d(a,y), \end{aligned}$$

and

$$\lim_{s \rightarrow +0} (\text{RHS}) = \int_{\mathbf{R}^d} dy G_d(a,y) e^{t\Delta_y} \delta_b(y).$$

Hence the conclusion holds. \square

Proof of Lemma 4.2. Note that $e^{t\Delta} \delta_b$ is the heat kernel with center b :

$$e^{t\Delta_y} \delta_b(y) = \frac{1}{(4\pi t)^{d/2}} \exp\left(-\frac{\|y-b\|^2}{4t}\right). \quad (\text{C.1})$$

Therefore the function $e^{t\Delta_y}\delta_b(y)$ depends only on t and the difference $y - b$. In addition, the function $G_d(b, y)$ depends only on $y - b$ as shown by formula (4.1). Then, by integration by substitution with $z = y - b$, we have

$$\begin{aligned} \int_{\mathbf{R}^d} dy G_d(b, y) e^{t\Delta_y}\delta_b(y) &= \int_{\mathbf{R}^d} dz G_d(0, z) e^{t\Delta_z}\delta_0(z) \\ &= \frac{1}{(4\pi t)^{d/2}} \int_{\mathbf{R}^d} dz G_d(z, 0) \exp\left(-\frac{\|z\|^2}{4t}\right). \end{aligned}$$

Clearly this value is independent of b . Furthermore, to show the boundedness of this value, we use the following estimate:

$$\begin{aligned} &\left| \int_{\mathbf{R}^d} dy G_d(b, y) e^{t\Delta_y}\delta_b(y) \right| \\ &\leq \frac{1}{(4\pi t)^{d/2}} \left(\int_{B_d[0,1]} + \int_{\mathbf{R}^d \setminus B_d[0,1]} \right) dz |G_d(z, 0)| \exp\left(-\frac{\|z\|^2}{4t}\right) \\ &\leq \frac{1}{(4\pi t)^{d/2}} \left(\int_{B_d[0,1]} dz |G_d(z, 0)| + \int_{\mathbf{R}^d \setminus B_d[0,1]} dz |G_d(z, 0)| \exp\left(-\frac{\|z\|^2}{4t}\right) \right). \quad (\text{C.2}) \end{aligned}$$

The first term in the parenthesis is bounded because of the argument in Section B. To estimate the second term, we note that $|G_d(z, 0)|$ depends only on $\|z\|$ and bounded by $c_d\|z\|$ for some constant $c_d > 0$ when $\|z\| \geq 1$. Therefore we have

$$\begin{aligned} \int_{\mathbf{R}^d \setminus B_d[0,1]} dz |G_d(z, 0)| \exp\left(-\frac{\|z\|^2}{4t}\right) &\leq s_d \int_1^\infty r^{d-1} dr \cdot c_d r \cdot \exp\left(-\frac{r^2}{4t}\right) \\ &= s_d c_d \int_1^\infty r^d \exp\left(-\frac{r^2}{4t}\right) dr < \infty. \end{aligned}$$

From these, the RHS of (C.2) is bounded. \square

Proof of Lemma 4.3. When $t \rightarrow +0$, the LHS tends to $G_d(a, b)$. By differentiating the LHS, we have

$$\begin{aligned} \frac{\partial}{\partial t}(\text{LHS}) &= \int_{\mathbf{R}^d} dy G_d(a, y) \Delta_y e^{t\Delta_y}\delta_b(y) \\ &= \int_{\mathbf{R}^d} dy \Delta_y G_d(a, y) e^{t\Delta_y}\delta_b(y) \\ &= \int_{\mathbf{R}^d} dy \delta_a(y) e^{t\Delta_y}\delta_b(y) \\ &= (e^{t\Delta}\delta_b)(a) \\ &= \frac{1}{(4\pi t)^{d/2}} \exp\left(-\frac{\|a-b\|^2}{4t}\right), \end{aligned}$$

where we use formula (C.1) in the last equality. Then, the conclusion follows. \square

Proof of Lemma 4.5. Set $\alpha := \|x - y\|$, which satisfies $0 < \alpha \leq D$. For preparation, we define a function g by

$$g(s) := \frac{1}{s^{d/2}} \exp\left(-\frac{\alpha^2}{4s}\right)$$

for $s > 0$. Since

$$g'(s) = \frac{1}{4s^{d/2+2}} \exp\left(-\frac{\alpha^2}{4s}\right) (\alpha^2 - 2ds),$$

the function g is unimodal and becomes maximum at $s = \frac{\alpha^2}{2d}$. Then, if we set $s_* = \frac{D^2}{2d}$, the function g is monotone decreasing on $[s_*, \infty)$. Therefore we have

$$g(s) \geq g(2s_*) \text{ for any } s \text{ with } s_* \leq s \leq 2s_*.$$

By using this inequality, we can derive the following estimate:

$$\begin{aligned} & \int_0^t \frac{1}{(4\pi s)^{d/2}} \exp\left(-\frac{\alpha^2}{4s}\right) ds \\ & \geq \frac{1}{(4\pi)^{d/2}} \left(\int_{s_*}^{2s_*} + \int_{2s_*}^t \right) g(s) ds \\ & \geq \frac{1}{(4\pi)^{d/2}} \left(s_* g(2s_*) + \exp\left(-\frac{\alpha^2}{8s_*}\right) \int_{2s_*}^t \frac{1}{s^{d/2}} ds \right) \\ & \geq \frac{1}{(4\pi)^{d/2}} \left(s_* g(2s_*) + \exp\left(-\frac{D^2}{8s_*}\right) \int_{2s_*}^t \frac{1}{s^{d/2}} ds \right) \\ & = \begin{cases} \frac{1}{(4\pi)^{d/2}} \left[\frac{d^{d/2-1}}{2D^{d-2}} \exp\left(-\frac{d\alpha^2}{4D^2}\right) + \frac{e^{-d/4}}{1-d/2} \left(\frac{1}{t^{d/2-1}} - \frac{d^{d/2-1}}{D^{d-2}} \right) \right] & (d \neq 2), \\ \frac{1}{(4\pi)^{d/2}} \left[\frac{d^{d/2-1}}{2D^{d-2}} \exp\left(-\frac{d\alpha^2}{4D^2}\right) + e^{-d/4} \log\left(\frac{td}{D^2}\right) \right] & (d = 2). \end{cases} \end{aligned} \quad (\text{C.3})$$

Thus the conclusion holds. \square